

Cerebral metabolite changes prior to and after antiretroviral therapy in primary HIV infection

Pt

Andrew C. Young
 Constantin T. Yiannoutsos, PhD
 Manu Hegde, MD, PhD
 Evelyn Lee
 Julia Peterson
 Rudy Walter
 Richard W. Price, MD
 Dieter J. Meyerhoff, PhD
 Serena Spudich, MD

Correspondence to
 Dr. Spudich:
 serena.spudich@yale.edu

ABSTRACT

Objective: We examined the longitudinal effects of primary HIV infection (PHI) and responses to early antiretroviral therapy (ART) on the brain using high-field magnetic resonance spectroscopy (MRS).

Methods: Cerebral metabolites were measured longitudinally with 4T proton MRS and assessed for ART effects in participants with PHI. Levels of glutamate (Glu), N-acetylaspartate (NAA), myo-inositol (MI), and choline-containing metabolites (Cho) were measured relative to creatine + phosphocreatine (Cr) in anterior cingulate, basal ganglia, frontal white matter, and parietal gray matter.

Results: Fifty-three participants recruited at median 3.7 months post HIV transmission were followed a median 6.0 months. A total of 23 participants initiated ART during follow-up. Prior to ART, increases per month were observed in Cho/Cr (slope = 0.0012, $p = 0.005$) and MI/Cr (slope = 0.0041, $p = 0.005$) in frontal white matter as well as increases in MI/Cr (slope = 0.0041, $p < 0.001$) and NAA/Cr (slope = 0.0024, $p = 0.030$) in parietal gray matter. After initiation of ART, prior positive slopes were no longer significantly different from zero, while Glu/Cr in basal ganglia decreased (slope = -0.0038, $p = 0.031$).

Conclusions: Early in HIV infection, increases of Cho/Cr and MI/Cr in treatment-naïve participants suggest progressive inflammation and gliosis in the frontal white matter and parietal gray matter, which is attenuated after initiation of ART. Elevated baseline Glu/Cr in basal ganglia may signal excitotoxicity; its subsequent stabilization and downward trajectory with ART may lend further support for early ART initiation. *Neurology®* 2014;83:1592–1600

GLOSSARY

ART = antiretroviral therapy; **CHI** = chronic HIV infection; **Cho** = choline-containing metabolites; **Cr** = creatine-containing metabolites; **Glu** = glutamate; **^1H -MRS** = proton magnetic resonance spectroscopy; **IQR** = interquartile range; **MI** = myo-inositol; **MPrAGE** = magnetization-prepared rapid gradient echo; **MR** = magnetic resonance; **NAA** = N-acetylaspartate; **PHI** = primary HIV infection; **TCA** = tricarboxylic acid; **TE** = echo time; **VOI** = volume of interest.

Proton magnetic resonance spectroscopy (^1H -MRS) can detect dynamic cerebral metabolite changes indicative of inflammation and neuronal injury in individuals with HIV.^{1–5} Biochemical cerebral metabolite evidence found in chronic HIV infection (CHI) are low N-acetylaspartate (NAA, a putative marker of neuronal health), high choline-containing metabolites (Cho, a marker of macrophage infiltration and inflammation), and high myo-inositol (MI, an astrocyte marker associated with astrocytosis, gliosis, and inflammation).^{1,4,5} Low glutamate (Glu) is also reported in CHI with cognitive impairment and is thought to reflect neuronal and glial cell dysfunction.⁶ Antiretroviral therapy (ART) offers limited reversibility^{7,8} even for CHI on stable long-term therapy,⁹ suggesting that early HIV invasion of the CNS^{10,11} and accrued neuronal damage¹² may contribute to the substantial prevalence of HIV-associated neurocognitive disorders in the era of ART.^{13,14} ^1H -MRS studies during primary HIV infection (PHI, the first year after HIV transmission) describes inflammation with trends of elevated Cho/creatinine-containing metabolites (Cr) and MI/Cr with potentially neurotoxic levels of Glx (combined glutamate and glutamine peak)^{10,15}; this corresponds with neuropathologic immune activation previously reported in PHI.^{16–20}

Editorial, page 1588

Supplemental data at Neurology.org

From Yale University (A.C.Y., S.S.), New Haven, CT; Indiana University (C.T.Y.), Indianapolis; and the University of California (M.H., E.L., J.P., R.W., R.W.P., D.J.M.), San Francisco.

Go to Neurology.org for full disclosures. Funding information and disclosures deemed relevant by the authors, if any, are provided at the end of the article.

To date, no ^1H -MRS study has examined the longitudinal effects of untreated early HIV in the brain, assessing for potentially deleterious effects that may be impacted by intervention with ART. Utilizing a 4T magnetic resonance (MR) scanner, we studied ART-naïve PHI participants prospectively, hypothesizing increases in Cho/Cr and MI/Cr. In participants who initiated ART during follow-up, we predicted reduction in markers of inflammation and excitotoxicity after treatment.

METHODS **Study participants and design.** Fifty-three PHI, 19 HIV-uninfected, and 18 CHI participants were recruited at the University of California San Francisco from 2005 to 2011. PHI was defined as recent infection within 12 months prior to enrollment, confirmed by the Serological Testing Algorithm for Recent HIV Seroconversion.²¹ Estimation of HIV transmission date used standard methods.²² CHI participants had a history of HIV diagnosis for at least 3 years. HIV-uninfected controls were matched to PHI for age, sex, and education level and recruited from the San Francisco community. Exclusion criteria included active neurologic illness, active usage of drugs of abuse, hepatitis B or C infection, and contraindications for MRI. MRS and laboratory data were collected at enrollment, 6 weeks, and every 6 months thereafter. ART start dates and regimens for PHI participants who initiated ART were recorded.

Standard protocol approvals, registrations, and patient consents. Study participant protocol was approved by UCSF and Yale institutional review boards. Written informed consent was obtained from all participants.

Magnetic resonance spectroscopy. ^1H -MRS examinations were performed on a Bruker (Billerica, MA) MedSpec 4T MR system with Siemens (Munich, Germany) Trio console in the Center for Imaging of Neurodegenerative Diseases at the San Francisco VA Medical Center. Short echo time (TE) single-volume stimulated-echo acquisition mode spectra (repetition time/TE/TM = 2,000/12/10 ms, spectral width = 2,000 Hz, 128 scans, vector size = 2,048 points, total time = 4:16 minutes) for 4 volumes of interest (VOIs) were selected on sagittal magnetization-prepared rapid gradient echo (MPRAGE) and axial turbo spin-echo images corresponding to different tissue types: (1) anterior cingulate cortex ($20 \times 20 \times 20 \text{ mm}^3$), (2) frontal white matter ($15 \times 25 \times 20 \text{ mm}^3$), (3) basal ganglia ($17 \times 35 \times 15 \text{ mm}^3$, centered on internal capsule and maximizing inclusion of caudate, putamen, and globus pallidus), and (4) parietal gray matter ($20 \times 20 \times 20 \text{ mm}^3$), maximizing gray matter by covering posterior cingulate (figure e-1 on the *Neurology*[®] Web site at Neurology.org). Proper repositioning of VOIs for repeat MRS was ascertained by matching VOI positions on sagittal T1 MPRAGE and axial T2-weighted images to baseline imaging. MR acquisition and processing are described in further detail in prior reports^{18,23} (note absolute concentrations were not calculated in the current study). The MR signal was normalized with Cr as presented in prior ^1H -MRS studies.^{1,3,8,10,24}

MRS data processing. For each metabolite peak, area under the curve was determined using the SITools software package,²⁵ which used a parametric model of known metabolites and modeled spectral components to fit all resonances and a nonparametric fit of the baseline. Metabolite areas were converted

to metabolite ratios—Glu/Cr, MI/Cr, NAA/Cr, and Cho/Cr—to correct for imager and localization method differences and uncontrollable experimental conditions such as gain instabilities, and further avoided the need to correct for different contributions of CSF to the analyzed MRS volumes. Spectra were reviewed when any of the metabolite ratios was greater than 1.5 SDs from the mean within each group. Reviewers were blinded to which metabolite deviated from the mean and were instructed to ensure that the software model fit the spectra accurately. When the model deviated from the observed spectra, parameters were adjusted in the SITools software to ensure an improved fit, and these data were used. Spectra were excluded when exhibiting poor signal-to-noise ratios or excessive water signal. Individual metabolite values were excluded if the optimized fitting did not yield satisfactory results. In the frontal white matter, 135/154 PHI spectra, 14/18 CHI spectra, and 17/19 HIV-uninfected spectra ($p = 0.471$, χ^2) were retained. In the parietal gray matter, 146/154 PHI spectra, 16/18 CHI spectra, and 19/19 HIV-uninfected spectra ($p = 0.316$, χ^2) were retained. In the anterior cingulate, 140/154 PHI spectra, 12/18 CHI spectra, and 17/19 HIV-uninfected spectra ($p = 0.009$, χ^2) were retained. The lower spectra count is attributable to delayed initiation of CHI anterior cingulate acquisition. In the basal ganglia, 135/154 PHI spectra, 16/18 CHI spectra, and 17/19 HIV-uninfected spectra were retained ($p = 0.966$, χ^2).

Laboratory data. Specimen sampling, processing, and laboratory studies. CSF, blood, and standardized medical and neurologic assessments were obtained as previously described.²⁶ Standard clinical CSF analyses and blood T-lymphocyte subsets were measured on fresh samples. HIV RNA levels were measured in previously frozen (-70°C) cell-free paired CSF and plasma samples in the same PCR run using the ultrasensitive Amplicor HIV Monitor V.1.5 (Roche Molecular Diagnostic Systems, Basel, Switzerland) or the Abbott RealTime HIV (Abbott Laboratories, Abbott Park, IL) assays.

Statistical analysis. Median follow-up times and times from enrollment to ART initiation were calculated via the Kaplan-Meier method. Baseline comparisons were made using the Kruskal-Wallis nonparametric test and the Fisher exact test. For ^1H -MRS, subject-specific metabolite signal areas from Glu, NAA, Cho, and MI relative to Cr areas were calculated for each VOI. Metabolite ratios between PHI, CHI, and HIV-uninfected controls were cross-sectionally compared for each VOI with the Kruskal-Wallis test. For the longitudinal analysis, a 2-phase linear mixed model utilizing an unstructured covariance matrix compared changes in pre-ART and post-ART metabolite ratios. A linear response curve was fitted to the time period for measurements absent treatment (ART-naïve) and a different linear response curve to the period after the start of treatment (ART-initiated) with the change in slopes reported as ART-interaction. ART-naïve and ART-initiated linear response curves were constrained to meet at the time of ART initiation (figure e-2). Starting values (intercepts) of the cerebral metabolite ratios were allowed to vary from participant to participant as were the linear slopes in the absence of treatment and after ART initiation. Statistical analyses were performed using SAS version 9.2 (SAS Institute, Cary, NC), STATA version 11.0 (StataCorp, College Station, TX), and graphics were generated by Graphpad (La Jolla, CA) Prism version 6.00.

RESULTS **Study participant characteristics.** A total of 53 men with PHI, 16 men and 2 women with CHI, and 19 HIV-uninfected men were studied

Table 1 Participant characteristics by group

	HIV-uninfected (n = 19)	Primary HIV infection (n = 53)	Chronic HIV infection (n = 18)	p Value
Male, %	100	100	89	0.038
Age, y	33 (28, 43)	37 (31, 45)	50 (39, 54)	0.002 ^{a,b}
Education, y	16 (14, 17)	16 (14, 16)	14 (12.5, 16)	0.058
Months post HIV diagnosis	NA	NA	93 (62.9, 216.1)	
Months post HIV transmission	NA	3.7 (2.1, 6.2)	NA	
CD4+, cells/mL	787 (710, 1,002)	542 (408, 741)	208 (104, 297)	<0.001 ^{c,d,e}
Plasma HIV RNA, log ₁₀ /mL	NA	4.59 (3.97, 5.00)	4.58 (3.75, 4.96)	0.932
CSF HIV RNA, log ₁₀ /mL	NA	2.62 (1.69, 3.33)	4.12 (2.35, 4.50)	0.001 ^d
CSF leukocytes, cells/ μ L	1 (1, 3)	6 (3, 11)	7.5 (2, 14)	<0.001 ^{b,c}

Abbreviation: NA = not applicable.

Values shown are median (Q1, Q3) unless otherwise indicated. Comparisons were made using Kruskal-Wallis nonparametric test for continuous variables. Fisher exact test was used for categorical variables.

^aPrimary HIV infection vs chronic HIV infection ($p < 0.05$).

^bHIV-uninfected vs chronic HIV infection ($p < 0.05$).

^cPrimary HIV infection vs HIV-uninfected ($p < 0.001$).

^dPrimary HIV infection vs chronic HIV infection ($p < 0.001$).

^eHIV-uninfected vs chronic HIV infection ($p < 0.001$).

cross-sectionally. Laboratory and demographic characteristics of the 3 groups are shown in table 1. At baseline, PHI was scanned at median 3.7 months post infection (interquartile range [IQR] 2.1–6.2) while CHI was scanned at median 93 months post diagnosis (IQR 62.9–216.1). Of the 53 PHI participants enrolled in the study, only 5 had a history of ART, of median duration 22 days prior to scanning. In the CHI group, 13 participants were ART-naive, 4 had less than a 2-week history of ART, and 1 had a 4-month proximal history of ART. Significant differences between groups in CD4+ T-cell count, CSF HIV RNA, and CSF leukocytes were identified in the baseline measures (table 1). As compared to HIV-uninfected participants, participants with PHI had lower median values in CD4+ T-cell count, measurable CSF HIV RNA, and higher CSF leukocytes.

Fifty-three participants with PHI were followed longitudinally with a total of 154 scans over a median 6.0 months (IQR 0–26.4). ART was initiated independently from the study by 23 of the 53 PHI participants at a median of 6.4 months (IQR 3.2–16.8) post HIV transmission. ART regimens consisted of 21 nucleoside reverse transcriptase inhibitors, 8 non-nucleoside reverse transcriptase inhibitors, 14 protease inhibitors, 4 integrase inhibitors, and 1 CCR5 entry inhibitor. Participants received ART for a median of 12.9 months (IQR 3.1–29.3) by the conclusion of follow-up.

Cross-sectional baseline cerebral metabolites. Group differences between PHI and HIV-uninfected participants were noted in parietal gray matter where PHI had lower Cho/Cr ($p = 0.007$) and MI/Cr ($p = 0.030$). PHI participants had higher Glu/Cr in the basal ganglia

relative to HIV-uninfected participants ($p = 0.027$). Comparisons between PHI and CHI revealed higher NAA/Cr in frontal white matter ($p = 0.003$) as well as higher NAA/Cr ($p = 0.014$) and MI/Cr ($p = 0.045$) in anterior cingulate in PHI. Finally, CHI compared to HIV-uninfected had lower NAA/Cr in frontal white matter ($p = 0.037$) and parietal gray matter ($p = 0.014$) as well as lower Glu/Cr in parietal gray matter ($p = 0.033$) (table 2 and figure 1). Kruskal-Wallis post-test results were not adjusted for multiple comparisons.

Cerebral metabolite changes prior to ART in PHI. Cho/Cr and MI/Cr in the frontal white matter and parietal gray matter increased prior to ART initiation. In frontal white matter, the trajectory of ART-naive Cho/Cr and MI/Cr increased at 0.0012/month ($p = 0.005$) and 0.0041/month ($p = 0.005$), respectively (figure 2, A and B). Similarly, in the parietal gray matter, ART-naive MI/Cr increased by 0.0041/month ($p < 0.001$) (figure 2C). In parietal gray matter, NAA/Cr increased by 0.0024/month ($p = 0.030$) (figure 2D).

Effects of ART on cerebral metabolite changes in PHI. Treatment with ART was associated with an apparent elimination of prior positive slopes for Cho/Cr and MI/Cr (i.e., slopes became insignificantly different from 0). In frontal white matter, the ART-initiated Cho/Cr slope decreased to 0.00017/month ($p = 0.654$) and ART-initiated MI/Cr slope decreased to 0.000797/month ($p = 0.578$) (figure 2, A and B). In parietal gray matter, the ART-initiated MI/Cr slope decreased to -0.0011/month ($p = 0.219$) (figure 2C). ART-interaction slopes trended toward significance for Cho/Cr and MI/Cr in frontal white

Table 2 Baseline cross-sectional cerebral metabolites

	Cho/Cr			MI/Cr			Glu/Cr			NAA/Cr		
	HIV-uninfected	PHI	CHI									
Frontal white matter												
Median	0.280	0.280	0.285	1.330	1.270	1.145	0.890	0.900	0.870	0.780	0.720	0.670
Standard error	0.0142	0.0062	0.0129	0.0547	0.0289	0.0410	0.0494	0.0222	0.0389	0.0584	0.0235	0.0386
Group analysis	<i>p</i> = 0.861			<i>p</i> = 0.952			<i>p</i> = 0.114			<i>p</i> = 0.012 ^a		
HIV– vs PHI	<i>p</i> = 0.584			<i>p</i> = 0.960			<i>p</i> = 0.185			<i>p</i> = 0.713		
PHI vs CHI	<i>p</i> = 0.841			<i>p</i> = 0.786			<i>p</i> = 0.175			<i>p</i> = 0.003 ^b		
HIV– vs CHI	<i>p</i> = 0.827			<i>p</i> = 0.751			<i>p</i> = 0.054			<i>p</i> = 0.037 ^a		
Parietal gray matter												
Median	0.200	0.190	0.190	1.330	1.240	1.170	0.890	0.810	0.810	1.150	1.070	0.990
Standard error	0.0036	0.0026	0.0058	0.0325	0.0153	0.0423	0.0360	0.0197	0.0355	0.0343	0.0200	0.0427
Group analysis	<i>p</i> = 0.028 ^a			<i>p</i> = 0.082			<i>p</i> = 0.060			<i>p</i> = 0.023 ^a		
HIV– vs PHI	<i>p</i> = 0.007 ^b			<i>p</i> = 0.030 ^a			<i>p</i> = 0.135			<i>p</i> = 0.064		
PHI vs CHI	<i>p</i> = 0.654			<i>p</i> = 1.0			<i>p</i> = 0.114			<i>p</i> = 0.086		
HIV– vs CHI	<i>p</i> = 0.116			<i>p</i> = 0.091			<i>p</i> = 0.033 ^a			<i>p</i> = 0.014 ^a		
Basal ganglia												
Median	0.230	0.240	0.245	1.070	1.120	1.000	0.605	0.610	0.630	0.720	0.780	0.720
Standard error	0.0131	0.0057	0.0081	0.0320	0.0226	0.0420	0.0426	0.0218	0.0444	0.0307	0.0200	0.0355
Group analysis	<i>p</i> = 0.462			<i>p</i> = 0.497			<i>p</i> = 0.079			<i>p</i> = 0.203		
HIV– vs PHI	<i>p</i> = 0.462			<i>p</i> = 0.303			<i>p</i> = 0.027 ^a			<i>p</i> = 0.465		
PHI vs CHI	<i>p</i> = 0.470			<i>p</i> = 0.815			<i>p</i> = 0.204			<i>p</i> = 0.082		
HIV– vs CHI	<i>p</i> = 0.201			<i>p</i> = 0.279			<i>p</i> = 0.880			<i>p</i> = 0.355		
Anterior cingulate												
Median	0.290	0.290	0.270	1.170	1.190	1.080	0.890	0.890	0.810	0.920	0.950	0.900
Standard error	0.0062	0.0036	0.0146	0.0321	0.0217	0.0388	0.0251	0.0139	0.0298	0.0273	0.0206	0.0428
Group analysis	<i>p</i> = 0.641			<i>p</i> = 0.145			<i>p</i> = 0.170			<i>p</i> = 0.046 ^a		
HIV– vs PHI	<i>p</i> = 0.583			<i>p</i> = 0.869			<i>p</i> = 0.875			<i>p</i> = 0.483		
PHI vs CHI	<i>p</i> = 0.486			<i>p</i> = 0.045 ^a			<i>p</i> = 0.065			<i>p</i> = 0.014 ^a		
HIV– vs CHI	<i>p</i> = 0.413			<i>p</i> = 0.176			<i>p</i> = 0.137			<i>p</i> = 0.096		

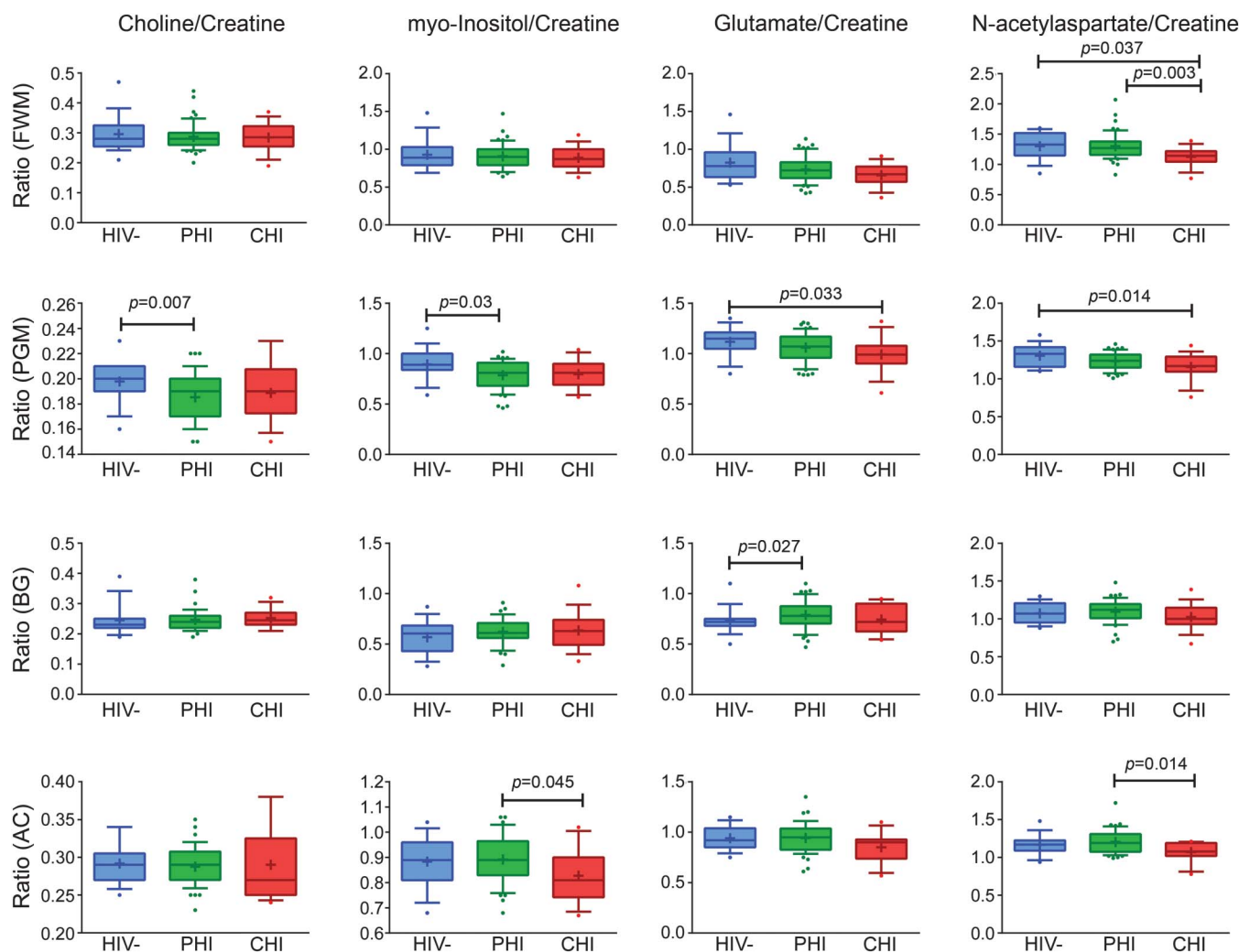
Abbreviations: CHI = chronic HIV infection; Cho = choline-containing metabolites; Cr = creatine-containing metabolites; Glu = glutamate; HIV– = HIV-uninfected; MI = myo-inositol; NAA = N-acetylaspartate; PHI = primary HIV infection.

Comparisons made using Kruskal-Wallis nonparametric test.

^a*p* < 0.05.

^b*p* < 0.01.

Figure 1 Cross-sectional magnetic resonance spectroscopy comparisons



Kruskal-Wallis comparison among cross-sectional groups: HIV-uninfected (HIV-), primary HIV infection (PHI), and chronic HIV infection (CHI) in frontal white matter (FWM), parietal gray matter (PGM), basal ganglia (BG), and anterior cingulate (AC). Kruskal-Wallis post-test results are not adjusted for multiple comparisons. Box and whiskers plot with whiskers at 10th–90th percentile.

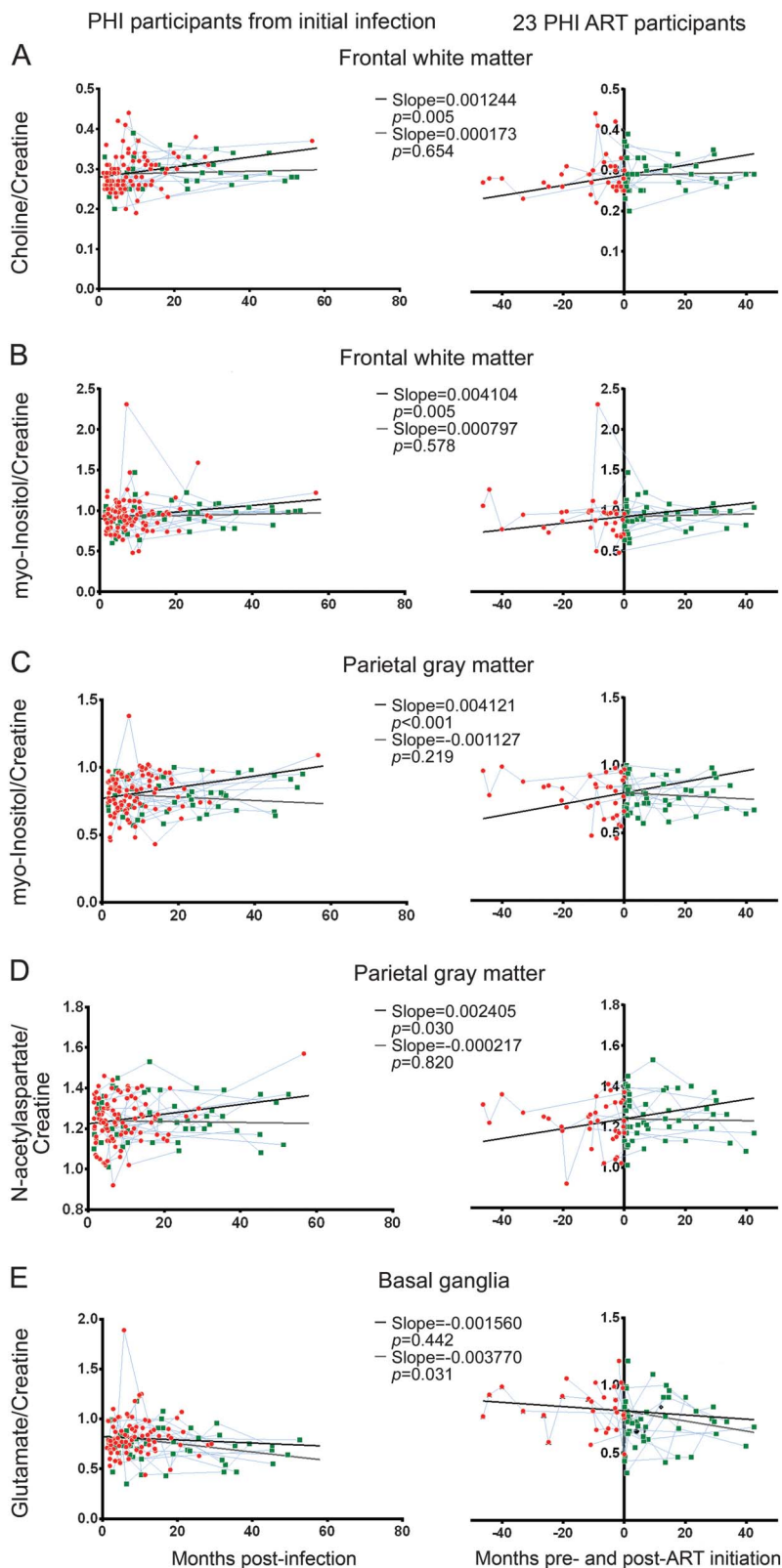
matter at $-0.0011/\text{month}$, $p = 0.073$ and $-0.0033/\text{month}$, $p = 0.077$, respectively, and was significant for MI/Cr in parietal gray matter with a slope of $-0.0052/\text{month}$, $p < 0.001$. Interestingly, the significantly elevated baseline Glu/Cr levels in basal ganglia decreased after ART initiation by $-0.0038/\text{month}$ ($p = 0.031$), though a nonsignificant ART-interaction slope ($-0.0022/\text{month}$, $p = 0.399$) is noted (figure 2E). Decreases in ART-initiated NAA/Cr slope in parietal gray matter were not significantly different from zero ($-0.0002/\text{month}$, $p = 0.820$) with an ART-interaction slope trending toward significance ($-0.0026/\text{month}$, $p = 0.074$) (figure 2D). Cerebral metabolite ratio slopes for each region can be found in table 3. p Values were not adjusted for multiple comparison.

DISCUSSION The presumed natural history of HIV neuropathogenesis is progressive inflammation in the

CNS leading to clinical neurologic dysfunction. Our findings suggest that inflammation and gliosis, the presumed substrates of later neurologic injury, initially manifest during the first year of HIV infection and worsen during early infection in the absence of treatment. In addition, our findings suggest that initiation of ART can alter this trajectory such that markers of inflammatory changes are no longer increasing, possibly limiting the extent of neurologic injury.

Our cross-sectional findings of lower Cho/Cr and MI/Cr in parietal gray matter in PHI when compared to HIV-uninfected participants may initially be puzzling. However, these results are consistent with our current understanding of the natural history of HIV infection. Longitudinal SIV/macaque studies report an initial elevation of Cho/Cr in acute infection that is subsequently reduced during the transition from acute to primary infection.^{27,28} Studies with human

Figure 2 Longitudinal cerebral metabolite ratios and results of linear mixed model analysis



Left column displays cerebral metabolite measurements in relationship to date of infection for all participants with primary HIV infection (PHI) and the right column displays measurements centered on date of antiretroviral therapy (ART) initiation for 23 ART participants. (A) Choline/creatinine ART-naive slopes increase in the frontal white matter. ART-initiated slope is not significantly different from zero. A similar pattern was seen in myo-inositol/creatinine in the

participants show a similar progression with elevated Cho/Cr at 16–17 days postexposure¹⁰ followed by lower Cho,¹⁵ consistent with our results of lower Cho/Cr and MI/Cr months after exposure. A plausible biological mechanism for the low Cho/Cr and MI/Cr in PHI may be the result of reduced viral load after the acute phase²⁴ and concomitant reduced membrane turnover and gliosis related to immune stabilization.

Following the prospective ART-naive PHI cohort revealed increases in metabolite levels suggestive of progressive inflammation: Cho/Cr and MI/Cr increased in the frontal white matter and MI/Cr increased in the parietal gray matter. The effect of ART in PHI was assessed with longitudinal mixed linear models, revealing attenuation of increasing inflammatory cerebral metabolite ratios Cho/Cr and MI/Cr with initiation of therapy (figure 2). While effective in preventing the increase of inflammatory cerebral metabolites, no significant reduction in inflammation markers was detected after ART initiation. A recent acute infection study has identified elevations of Cho/Cr in the basal ganglia at 14 days postexposure and its subsequent reduction to control levels with 6 months of ART.²⁹ The reduction of basal ganglia Cho/Cr in that study may be related to the earlier initiation of ART than in our study. It is also possible that this is a region-specific observation, as the study also noted a Cho/Cr elevation in the occipital gray matter at baseline that was not reduced upon ART initiation. Our results suggest attenuation but not reversibility of Cho/Cr and MI/Cr in frontal white matter and parietal gray matter. Reversibility of Cho/Cr and MI/Cr may occur beyond follow-up, but this is unlikely as persistent neuroinflammation has been reported in chronic infection on stable ART.⁹

An early infection study with 8 individuals scanned within months of initial HIV exposure reported low NAA in the frontal cortical gray matter as compared to seronegative controls. All individuals reported symptoms of acute HIV syndrome and 5 additionally reported severe headaches, numbness in extremities, and difficulty thinking clearly.³⁰ In predominantly less symptomatic acute infection studies, no significant

frontal white matter (B) and parietal gray matter (C). (D) N-acetylaspartate/creatinine ART-naive slope increases in the parietal gray matter; ART-initiated slope is not significantly different from zero. (E) Glutamate/creatinine ART-naive slope is not significantly different from zero in the basal ganglia. However, ART-initiated slope is significantly negative. For all graphs, red circles represent ART-naive measurements, black lines represent ART-naive slope, green squares represent post-ART measurements, and blue lines connect participants' metabolite ratios longitudinally. Gray lines represent ART-initiated slope beginning at 6.4 months (median time of ART initiation) in the left column and begin at 0.0 months in the right column.

Table 3 Change in primary HIV infection cerebral metabolite ratios

	ART-naïve		ART-interaction		ART-initiated	
	Slope	p Value	Slope	p Value	Slope	p Value
Frontal white matter						
Cho/Cr	0.001244	0.005	-0.001083	0.073	0.000173	0.654
MI/Cr	0.004104	0.005	-0.003293	0.077	0.000797	0.578
NAA/Cr	0.002288	0.334	-0.002557	0.429	-0.000303	0.900
Glu/Cr	0.005521	0.119	-0.004073	0.414	0.001465	0.708
Parietal gray matter						
Cho/Cr	0.000238	0.269	-0.000217	0.402	0.000008	0.968
MI/Cr	0.004121	<0.001	-0.005243	<0.001	-0.001127	0.219
NAA/Cr	0.002405	0.030	-0.002643	0.074	-0.000217	0.820
Glu/Cr	0.001421	0.272	-0.002730	0.079	-0.001300	0.267
Basal ganglia						
Cho/Cr	-0.000347	0.481	0.000364	0.528	0.000017	0.968
MI/Cr	-0.003033	0.211	0.001023	0.743	-0.001993	0.375
NAA/Cr	0.000351	0.904	-0.001733	0.656	-0.001387	0.573
Glu/Cr	-0.001560	0.442	-0.002210	0.399	-0.003770	0.031
Anterior cingulate						
Cho/Cr	0.000316	0.336	0.000134	0.768	0.000451	0.146
MI/Cr	0.000546	0.709	-0.000021	0.992	0.000524	0.710
NAA/Cr	0.000698	0.496	-0.002210	0.122	-0.001517	0.118
Glu/Cr	0.001127	0.370	0.000498	0.775	0.001625	0.157

Abbreviations: ART = antiretroviral therapy; Cho = choline-containing metabolites; Cr = creatine-containing metabolites; Glu = glutamate; MI = myo-inositol; NAA = N-acetylaspartate.

ART-naïve, ART-interaction, and ART-initiated slopes and p values were determined by 2-phase linear mixed model analysis from longitudinal primary HIV infection cerebral metabolite measurements.

differences in baseline NAA/Cr were identified,^{10,29} though this may be limited by sample size. Similarly, we report no significant differences in baseline NAA/Cr in PHI as compared to HIV-uninfected controls, but low NAA/Cr in parietal gray matter trended toward significance ($p = 0.064$). Interestingly, we found increasing NAA/Cr in this brain region, which may suggest recovery after an initial drop in NAA/Cr that has been reported in acute infection in SIV³¹ and early infection in humans.³⁰ Evidence for recovery of NAA/Cr is also reported in acute infection studies with increases (greatest in first months post infection) in NAA/Cr in frontal gray matter, frontal white matter, and occipital gray matter despite not detecting significant differences at baseline.²⁹ Furthermore, baseline NAA/Cr in basal ganglia was significantly elevated in Fiebig III/IV when compared to Fiebig I/II,²⁹ which provides additional context for a temporal relationship of recovering NAA/Cr. We detected increases of NAA/Cr in the ART-naïve condition, which implies that NAA/Cr recovery in early infection may not be dependent on ART, and hypothesize that the lack of significance in ART-initiated slope can be

attributable to the later timeframe rather than the effect of therapy.

In the basal ganglia, Glu/Cr was elevated prior to ART and significantly declined after initiation of therapy (figure 2E). Elevated Glu/Cr prior to ART is concerning for Glu excitotoxicity via excessive NMDA receptor stimulation by increasing Glu production and release from HIV-infected macrophages or microglia^{32,33} in addition to dysregulation of astrocyte glutamate reuptake.³⁴ Our data suggest that ART may control viral presence and limit Glu excitotoxicity. Alternatively, nucleoside analog reverse transcriptase inhibitors, which 21 of 23 participants received, are known to cause mitochondrial oxidative stress,³⁵ which may result in reduced Glu synthesis from the tricarboxylic acid (TCA) cycle. Diminished resting cerebral blood flow in the lenticular nucleus of 33 predominantly ART-treated participants in early HIV infection may further suggest reduced TCA cycle metabolism.³⁶ Although ART appears to limit Glu excess, mitochondrial toxicity may play a role and must be considered in early adoption of ART. Regardless of the mechanism of Glu reduction, the

elevation of Glu/Cr in basal ganglia prior to ART may suggest utility of ¹H-MRS as initial screening for neuronal damage prior to NAA/Cr changes.

One limitation of our study is that we assessed metabolite-to-Cr ratios rather than absolute metabolite concentrations. Absolute cerebral metabolite concentration analysis may overcome possible confounds resulting from Cr level alterations in HIV infection or between subject groups.^{37,38} It is not known whether absolute concentrations of Cr may change during the early stages of infection, and thus characterization of absolute metabolites over time should be considered in future studies. Readers should note that baseline cross-sectional findings may be attributable to HIV and non-HIV influences. For example, despite matching, there is a nonsignificant but notable 4-year difference in median age between the PHI and HIV– cohort and significant age differences with CHI. Sufficient longitudinal HIV-uninfected control data were not obtained to compare to with PHI data, thus observed PHI trends cannot be conclusively stated to be the result of infection rather than a general process such as aging. Furthermore, due to the large number of statistical tests performed in this study, the evidence provided by this data need to be carefully weighed as *p* values were not adjusted for multiplicity, inflating the probability of false-positive type 1 errors. If adjusted for multiple comparisons, only our major findings of increasing MI/Cr in parietal gray matter prior to ART and its subsequent attenuation by ART remain significant. Despite these limitations, our study presents novel hypothesis-generating data for ART-naïve and ART-initiated longitudinal changes in ¹H-MRS cerebral metabolite markers in a large and well-characterized PHI cohort.

Our observations consistently show longitudinal increases of the inflammatory brain metabolite markers Cho/Cr and MI/Cr that suggest worsening inflammation during early untreated HIV. ART initiation during the first year of infection attenuated the increase of these inflammatory cerebral markers, but it did not appear to reverse them within the follow-up period. It is unknown whether after longer-term treatment and follow-up, ART initiated during early infection might reduce or eliminate inflammation, which has been observed in the setting of chronic, treated HIV infection. However, early diagnosis and adoption of ART is associated with low prevalence of neurocognitive impairment, providing further support for early intervention.³⁹ Our MRS-based observations suggest that early ART initiation may be advisable to prevent neurologic dysfunction by slowing and possibly halting HIV-associated neuropathology.

AUTHOR CONTRIBUTIONS

Andrew Young drafted the manuscript, organized and analyzed the laboratory and MRS dataset, and contributed to the statistical analysis. Constantin T. Yiannoutsos performed the longitudinal statistical analysis and

edited the manuscript. Manu Hegde contributed to the study design, processed MRS data, and reviewed the manuscript. Evelyn Lee recruited and scheduled the subjects, assisted with laboratory and MRS data collection, and reviewed the manuscript. Julia Peterson recruited and scheduled the subjects, assisted with laboratory and MRS data collection, and reviewed the manuscript. Rudy Walter acquired and processed MRS data and reviewed the manuscript. Richard W. Price contributed to the study design, recruited and assessed subjects, and edited the manuscript. Dieter J. Meyerhoff contributed to the study design, developed the MRS imaging protocol, and edited the manuscript. Serena Spudich developed the study design, recruited and assessed subjects, supported the studies, and edited the manuscript.

ACKNOWLEDGMENT

The authors thank the participants who volunteered for these studies and the staff at the UCSF Options Study and Magnet/San Francisco AIDS Foundation for collaboration and referral of study participants.

STUDY FUNDING

Supported by the NIH (grants R01 MH081772, K23 MH074466, P01 AI071713, M01 RR0008336), the Yale School of Medicine Summer Research grant, and the resources and use of facilities at the San Francisco Veterans Administration Medical Center.

DISCLOSURE

A. Young and C. Yiannoutsos report no disclosures relevant to the manuscript. M. Hegde receives salary support from the Epilepsy Study Consortium and has received an honorarium from LEK Consulting. E. Lee, J. Peterson, and R. Walter report no disclosures relevant to the manuscript. R. Price has received an honorarium and travel expenses for presentation at a scientific meeting from AbbVie Inc. and has served as a consultant to Merck. D. Meyerhoff reports no disclosures relevant to the manuscript. S. Spudich has received an honorarium and travel expenses for presentation at a scientific meeting from AbbVie Inc. Go to Neurology.org for full disclosures.

Received January 5, 2014. Accepted in final form June 16, 2014.

REFERENCES

1. Meyerhoff DJ, MacKay S, Poole N, Dillon WP, Weiner MW, Fein G. *N*-acetylaspartate reductions measured by ¹H MRSI in cognitively impaired HIV-seropositive individuals. *Magn Reson Imaging* 1994; 12:653–659.
2. Yiannoutsos CT, Ernst T, Chang L, et al. Regional patterns of brain metabolites in AIDS dementia complex. *Neuroimage* 2004;23:928–935.
3. Sacktor N, Skolasky RL, Ernst T, et al. A multicenter study of two magnetic resonance spectroscopy techniques in individuals with HIV dementia. *J Magn Reson Imaging* 2005;21:325–333.
4. Chang L, Ernst T, Leonido-Yee M, Walot I, Singer E. Cerebral metabolite abnormalities correlate with clinical severity of HIV-1 cognitive motor complex. *Neurology* 1999;52:100–108.
5. Meyerhoff DJ, Bloomer C, Cardenas V, Norman D, Weiner MW, Fein G. Elevated subcortical choline metabolites in cognitively and clinically asymptomatic HIV+ patients. *Neurology* 1999;52:995–991003.
6. Ernst T, Jiang CS, Nakama H, Buchthal S, Chang L. Lower brain glutamate is associated with cognitive deficits in HIV patients: a new mechanism for HIV-associated neurocognitive disorder. *J Magn Reson Imaging* 2010; 32:1045–1053.
7. Stankoff B, Tourbah A, Suarez S, et al. Clinical and spectroscopic improvement in HIV-associated cognitive impairment. *Neurology* 2001;56:112–115.

8. Chang L, Ernst T, Witt MD, et al. Persistent brain abnormalities in antiretroviral-naïve HIV patients 3 months after HAART. *Antivir Ther* 2003;8:17–26.
9. Harezlak J, Buchthal S, Taylor M, et al. Persistence of HIV-associated cognitive impairment, inflammation, and neuronal injury in era of highly active antiretroviral treatment. *AIDS* 2011;25:625–633.
10. Valcour V, Chalermchai T, Sailasuta N, et al. Central nervous system viral invasion and inflammation during acute HIV infection. *J Infect Dis* 2012;206:275–282.
11. Davis LE, Hjelle BL, Miller VE, et al. Early viral brain invasion in iatrogenic human immunodeficiency virus infection. *Neurology* 1992;42:1736–1739.
12. Kaul M, Zheng J, Okamoto S, Gendelman HE, Lipton SA. HIV-1 infection and AIDS: consequences for the central nervous system. *Cell Death Differ* 2005;12(suppl 1): 878–892.
13. Heaton RK, Clifford DB, Franklin DR Jr, et al. HIV-associated neurocognitive disorders persist in the era of potent antiretroviral therapy: CHARTER Study. *Neurology* 2010;75:2087–2096.
14. Simioni S, Cavassini M, Annoni JM, et al. Cognitive dysfunction in HIV patients despite long-standing suppression of viremia. *AIDS* 2010;24:1243–1250.
15. Lentz MR, Kim WK, Kim H, et al. Alterations in brain metabolism during the first year of HIV infection. *J Neurovirol* 2011;17:220–229.
16. Cinque P, Brew BJ, Gisslen M, Hagberg L, Price RW. Cerebrospinal fluid markers in central nervous system HIV infection and AIDS dementia complex. *Handb Clin Neurol* 2007;85:261–300.
17. Hagberg L, Cinque P, Gisslen M, et al. Cerebrospinal fluid neopterin: an informative biomarker of central nervous system immune activation in HIV-1 infection. *AIDS Res Ther* 2010;7:15.
18. Peluso MJ, Meyerhoff DJ, Price RW, et al. Cerebrospinal fluid and neuroimaging biomarker abnormalities suggest early neurological injury in a subset of individuals during primary HIV infection. *J Infect Dis* 2013;207: 1703–1712.
19. Spudich S, Gisslen M, Hagberg L, et al. Central nervous system immune activation characterizes primary human immunodeficiency virus 1 infection even in participants with minimal cerebrospinal fluid viral burden. *J Infect Dis* 2011;204:753–760.
20. Letendre SL, Zheng JC, Kaul M, et al. Chemokines in cerebrospinal fluid correlate with cerebral metabolite patterns in HIV-infected individuals. *J Neurovirol* 2011;17:63–69.
21. Zetola NM, Pilcher CD. Diagnosis and management of acute HIV infection. *Infect Dis Clin North Am* 2007;21:19–48.
22. Lindblad S, Thorstensson R, Karlsson AC, et al. Diagnosis of primary HIV-1 infection and duration of follow-up after HIV exposure: Karolinska Institute Primary HIV Infection Study Group. *AIDS* 2000;14:2333–2339.
23. Abe C, Mon A, Durazzo TC, Pennington DL, Schmidt TP, Meyerhoff DJ. Polysubstance and alcohol dependence: unique abnormalities of magnetic resonance-derived brain metabolite levels. *Drug Alcohol Depend* 2013;130:30–37.
24. Lindblad S, Karlsson AC, Mittler J, et al. Viral dynamics in primary HIV-1 infection: Karolinska Institute primary HIV infection study group. *AIDS* 2000;14:2283–2291.
25. Soher BJ, Young K, Govindaraju V, Maudsley AA. Automated spectral analysis III: application to in vivo proton MR spectroscopy and spectroscopic imaging. *Magn Reson Med* 1998;40:822–831.
26. Spudich SS, Nilsson AC, Lollo ND, et al. Cerebrospinal fluid HIV infection and pleocytosis: Relation to systemic infection and antiretroviral treatment. *BMC Infect Dis* 2005;5:98.
27. Fuller RA, Westmoreland SV, Ratai E, et al. A prospective longitudinal in vivo ¹H MR spectroscopy study of the SIV/macaque model of neuroAIDS. *BMC Neurosci* 2004;5:10–10.
28. Ratai EM, Pilkenton SJ, Greco JB, et al. In vivo proton magnetic resonance spectroscopy reveals region specific metabolic responses to SIV infection in the macaque brain. *BMC Neurosci* 2009;10:63.
29. Sailasuta N, Ross W, Ananworanich J, et al. Change in brain magnetic resonance spectroscopy after treatment during acute HIV infection. *PLoS One* 2012;7:e49272.
30. Lentz MR, Kim WK, Lee V, et al. Changes in MRS neuronal markers and T cell phenotypes observed during early HIV infection. *Neurology* 2009;72:1465–1472.
31. Greco JB, Westmoreland SV, Ratai EM, et al. In vivo ¹H MRS of brain injury and repair during acute SIV infection in the macaque model of neuroAIDS. *Magn Reson Med* 2004;51:1108–1114.
32. O'Donnell LA, Agrawal A, Jordan-Sciutto KL, Dichter MA, Lynch DR, Kolson DL. Human immunodeficiency virus (HIV)-induced neurotoxicity: roles for the NMDA receptor subtypes. *J Neurosci* 2006;26:981–990.
33. Erdmann NB, Whitney NP, Zheng J. Potentiation of excitotoxicity in HIV-1 associated dementia and the significance of glutaminase. *Clin Neurosci Res* 2006;6: 315–328.
34. Wang Z, Pekarskaya O, Bencheikh M, et al. Reduced expression of glutamate transporter EAAT2 and impaired glutamate transport in human primary astrocytes exposed to HIV-1 or gp120. *Virology* 2003;312:60–73.
35. Kohler JJ, Lewis W. A brief overview of mechanisms of mitochondrial toxicity from NRTIs. *Environ Mol Mutagen* 2007;48:166–172.
36. Ances BM, Sisti D, Vaida F, et al. Resting cerebral blood flow: a potential biomarker of the effects of HIV in the brain. *Neurology* 2009;73:702–708.
37. Ernst T, Itti E, Itti L, Chang L. Changes in cerebral metabolism are detected prior to perfusion changes in early HIV-CMC: a coregistered ¹H MRS and SPECT study. *J Magn Reson Imaging* 2000;12:859–865.
38. Schifitto G, Deng L, Yeh TM, et al. Clinical, laboratory, and neuroimaging characteristics of fatigue in HIV-infected individuals. *J Neurovirol* 2011;17:17–25.
39. Crum-Cianflone NF, Moore DJ, Letendre S, et al. Low prevalence of neurocognitive impairment in early diagnosed and managed HIV-infected persons. *Neurology* 2013;80:371–379.